catalysts

MDPI

Article

New Co and Mn Catalysts Bearing ONO Ligands Containing Nucleophile for the Coupling of CO_2 and Propylene Oxide

Mónica Viciano [1,2,*,†], Bianca K. Muñoz [1,3,*,†], Ennio Zangrando [4], Cyril Godard [5], Sergio Castillón [6], Mª Dolores Blanco González [7], Mónica García-Ruíz [7] and Carmen Claver [1,5]

1 Technologic Centre of Catalonia (EURECAT), C/Marcel·lí Domingo s/n, 43007 Tarragona, Spain
2 Plastics Technology Centre (AIMPLAS), Paterna Technologic Park, C/ Gustave Eiffel, 4. Paterna, 46980 Valencia, Spain
3 Materials Science and Engineering Area, University Rey Juan Carlos, ESCET, C/ Tulipán s/n, 28933 Móstoles, Spain
4 Department of Chemical and Pharmaceutical Sciences, University of Trieste, Via Giorgieri 1, 34127 Trieste, Italy
5 Department of Physical and Inorganic Chemistry, University Rovira and Virgili, C/Marcel·lí Domingo s/n, Campus Sescelades, 43007 Tarragona, Spain
6 Department of Analytical and Organic Chemistry, University Rovira and Virgili, IC/Marcel·lí Domingo s/n, Campus Sescelades, 43007 Tarragona, Spain
7 Repsol Technological Center, 28931 Móstoles, Spain
* Correspondence: mviciano@aimplas.es (M.V.); bianca.munoz@urjc.es (B.K.M.); Tel.: +34-663-459-596 (M.V.)
† B.K.M. and M.V. want to dedicate this paper to C.C. on the occasion of her retirement.

Abstract: A series of novel ONO ligands bearing an ionic pendant-armed (hereinafter indicated as ONONu, where Nu corresponds to an anionic nucleophile) were synthesized, characterized, and successfully coordinated to cobalt and manganese precursors. New air-stable cobalt (III) complexes (**1**–**6**) and manganese (II) complexes (**7** and **8**) were obtained and characterized. Single crystal X-ray diffraction analysis of the Co(III) compound **5** confirmed the presence of two quaternized ligands coordinated to the metal and iodide as counterion. These novel complexes were revealed to be active catalysts in the coupling reaction of carbon dioxide and propylene oxide (PO) in different degrees of success. Among these, the manganese complex **8** afforded the best results towards the formation of propylene carbonate (PC) with a productivity of 256 kg PC/(kg cat·h), achieving a TON of 4860.

Keywords: carbon dioxide; CO_2 utilization; homogeneous catalysis; cyclic carbonates; ONO ligands; CO_2 coupling reactions; ionic pendant-armed ligands; manganese catalysts; cobalt catalysts

check for updates

Citation: Viciano, M.; Muñoz, B.K.; Zangrando, E.; Godard, C.; Castillón, S.; Blanco González, M.D.; García-Ruíz, M.; Claver, C. New Co and Mn Catalysts Bearing ONO Ligands Containing Nucleophile for the Coupling of CO_2 and Propylene Oxide. *Catalysts* **2022**, *12*, 1443. https://doi.org/10.3390/catal12111443

Academic Editor: Antonio Monopoli

Received: 24 September 2022
Accepted: 1 November 2022
Published: 15 November 2022

1. Introduction

Over the last decade, the transformation of carbon dioxide into high-added-value products has received much attention as part of the carbon capture and utilization strategy (CCU) where CO_2 can be used as an abundant and cheap carbon source for organic synthesis and industrial processes [1,2]. The reaction between CO_2 and epoxides yielding the corresponding cyclic carbonates is of particular interest as a 100% atom economical process and the interesting properties of the product such as high boiling point, low toxicity and odorless, were highlighted for their use as green solvents in industrial processes [3]. Moreover, they can be used as aprotic polar solvents, intermediates for organic and polymeric synthesis, as well as solvents for electrolytes in lithium-ion batteries [4,5].

Several homogeneous and heterogeneous catalytic systems were developed for the synthesis of cyclic organic carbonates from CO_2 and epoxides. In particular, homogeneous complexes involving Co [6,7], Al [8–10], Zn [11,12], Mn [13], Fe [14] and Cr [6] are the most efficient species (Figure 1). One of the best systems reported for carbon dioxide and 1,2-epoxides coupling was reported by Kleij and coworkers and consists of an Al complex bearing an amino-tris (phenolate) ligand scaffold (Figure 1, catalyst **B**). These authors

reported a TOF of 26,000 h^{-1} under very mild conditions in the presence of a co-catalyst (a quaternary ammonium salt) [8,15]. The chromium complex reported by Paddock and Nguyen (Figure 1, catalyst **A**) exhibits a moderate activity under mild conditions [16]. Mono- and di-nuclear iron catalysts were also reported as efficient catalysts and the TON achieved are among the best reported for propylene oxide (Figure 1, catalyst **D**,**E**) [17,18]. Manganese complexes are less common in this reaction, but their low toxicity and low price made them interesting alternatives for this reaction (Figure 1, catalyst **C**,**F**–**H**) [13,19–21]. Previous results obtained in our group [21] (Figure 1, catalyst **H**) showed that manganese complexes modified with ONO ligands can provide high catalytic activity (TOF of 1600 h^{-1}) in the formation of propylene carbonate in the presence of a co-catalyst.

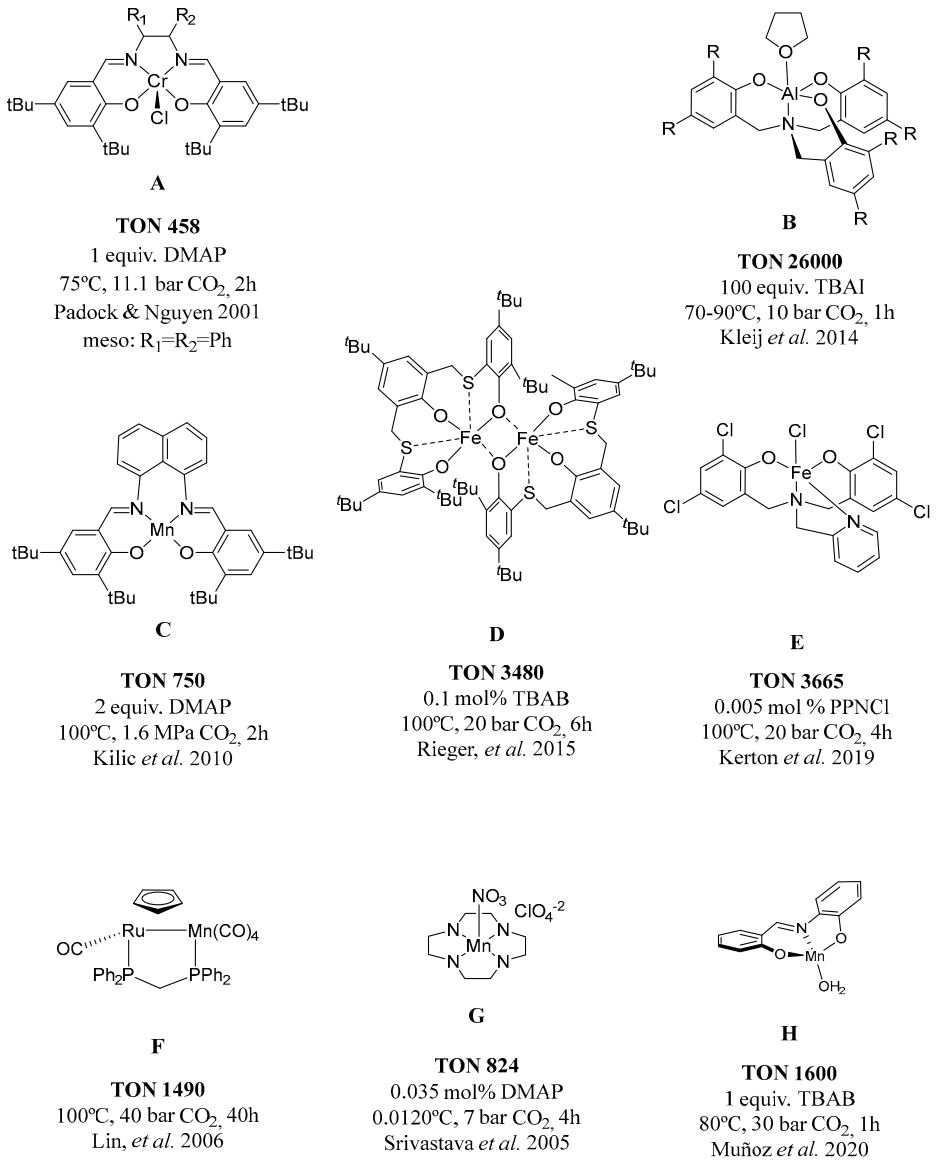

Figure 1. Selected catalytic systems developed for the synthesis of cyclic organic carbonates from CO_2 and epoxides.

From a mechanistic point of view, the coupling of one molecule of epoxide with CO_2 is followed by an internal cyclisation step to form a cyclic carbonate. This process involves two catalytic sites: Lewis acid and Lewis base or nucleophilic center. These two sites could be combined in the same molecule to afford a cooperative catalyst. This synergistic action of the electrophile with a nucleophile was described in bifunctional catalysts including a Lewis acid metal center with a quaternary ammonium salt [22], a quaternary phosphonium

salt [23] or a quaternary onium salt [24], which act as nucleophilic centers (Figure 2). In these cases, the ligands usually present a planar tetradentate dianionic structure (*salen*-type ligands) [25–29].

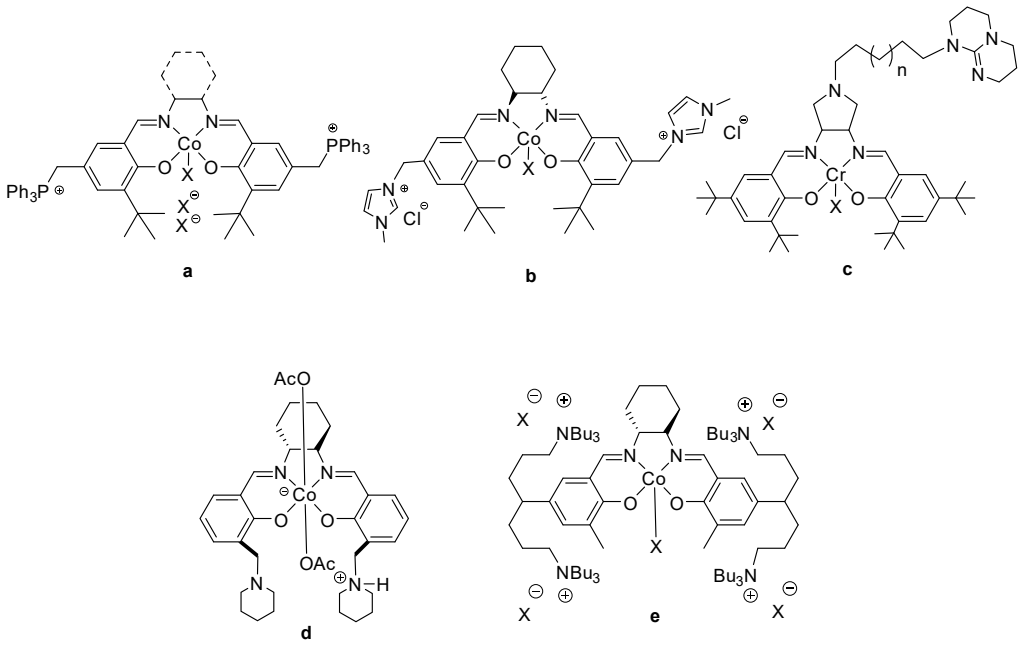

Figure 2. Bifunctional catalysts reported for CO_2/epoxides coupling reactions. Catalyst prepared by: (**a**) He et al., 2008 [23] and Jing et al., 2009 [24]; (**b**) Jing et al., 2009 [24]; (**c**) Sun et al., 2008 [22]; (**d**) Nozaki et al., 2006 [30]; (**e**) Lee, et al., 2008 [31].

Among the bifunctional examples depicted in Figure 2, the most active catalyst for the coupling reaction of CO_2 with epoxides is the chromium complex c, which afforded a TOF of 1936 h^{-1} in neat epoxide at 80 °C and 2.0 MPa of CO_2. The bifunctional salicylidene cobalt complexes with piperidinium moieties (Figure 2d) [30] and with quaternary ammonium groups (Figure 2e) [31] are among the most active catalysts for the formation of polycarbonates.

Herein, we report a new generation of catalysts bearing tridentate ligands with a cocatalyst in their structure (Figure 3). The synthesis of novel pendant-armed ligands ONONu and of the corresponding Co(III) and Mn(II) catalysts bearing this ligand are described. These new cobalt and manganese complexes were revealed as very active in the coupling reaction of CO_2 and propylene oxideto afford cyclic carbonates.

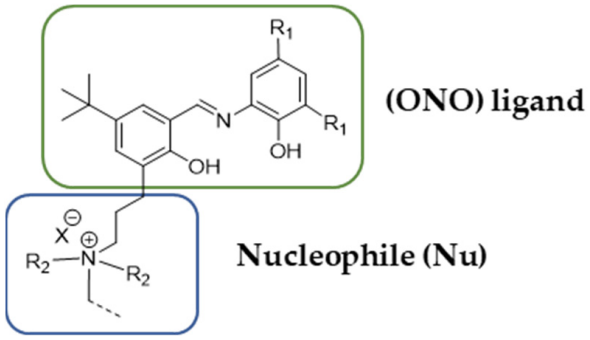

Figure 3. General structure of (ONONu) ligands.

2. Results and Discussion

2.1. Preparation and Characterization of (ONONu) Ligands

The synthesis of the ONONu ligands was performed in two steps from 5-tert-butyl-3-(3-(diethylamino)propyl)-2-hydroxybenzaldehyde (**F1**), affording the products in overall quantitative yields. The fragment **F1** was previously prepared according to a procedure in the literature [32]. Then, **F1** or **F2** was condensed with the corresponding aminoalcohol in dry ethanol during 2 h at 80 °C to afford the desired ligands (**L1**–**L4**) (Scheme 1).

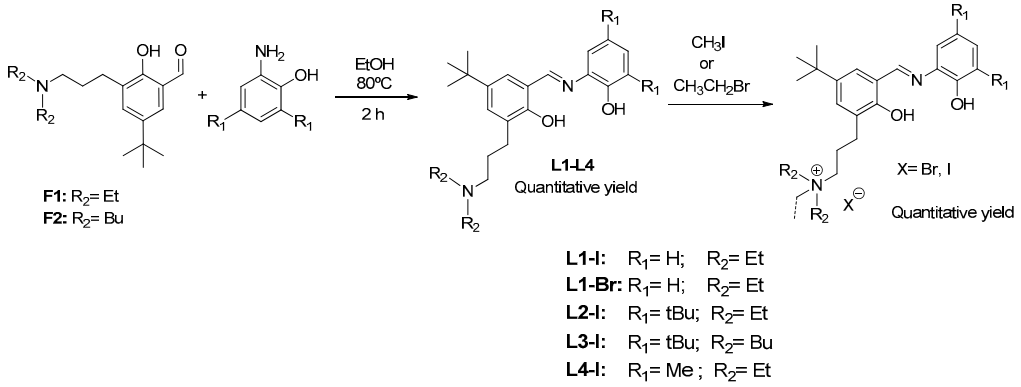

Scheme 1. Synthesis of ONONu ligands (**L1**–**L4**)-**X**.

The amine functions of ligands (**L1**–**L4**) were subsequently quaternized by reaction with an excess of iodomethane or bromoethane (**L1-X**; X=I, Br) in CH_2Cl_2 at room temperature for 3 h (Scheme 1). When the formation of the quaternized ligands was achieved, a singlet signal around 2.90 ppm was observed in the ^{1}H NMR (integration, 3H) in the case of methylated ligands, while after quaternization using bromoethane (only with ligand (**L1**)), ethyl group appeared at ca. 3.10 ppm (t, CH_3 group) and a multiplet around 4.00 ppm (CH_2 group). Moreover, in the ^{1}H NMR spectrum of **L1**, the broad signal at δ 13.95 ppm corresponding to –OH proton shifted to 14.23 ppm when the ligand was quaternized. All the ligands synthesized were characterized by ^{1}H and ^{13}C {1H} NMR, FTIR and UV-Vis spectroscopy.

2.2. Preparation and Characterization of Cobalt and Manganese Complexes

2.2.1. Preparation and Characterization of Co(III) (ONONu) Complexes

A series of novel Co(III) catalysts bearing the newly prepared ONONu ligands were synthetized. The synthesis of these complexes was carried out by reacting $Co(OAc)_2{\cdot}4H_2O$ with the corresponding ligand in ethanol, followed by oxidation with an excess of acetic acid (**1**–**6**) under aerobic conditions (Scheme 2). The prepared complexes were obtained as air-stable brown powders in moderate yields (43–55%).

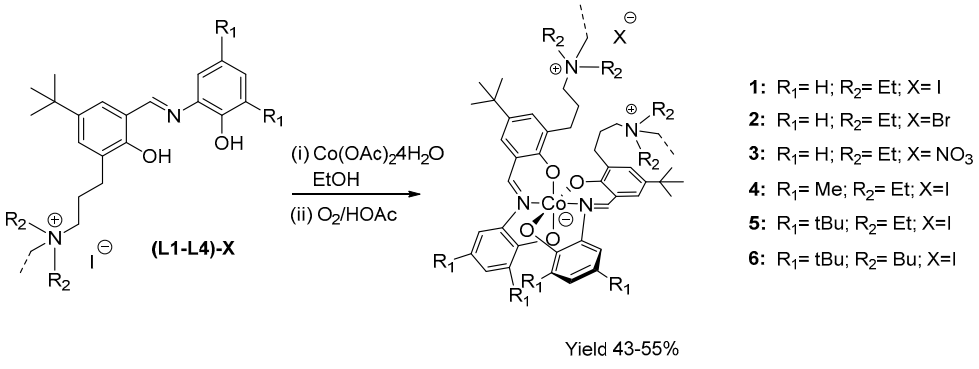

Scheme 2. Synthesis of Co(III)(ONONu) complexes (**1**–**6**).

These cobalt compounds were characterized by NMR spectroscopy, mass spectroscopy (ESI-TOF), and single crystal X-ray diffraction. Mass spectra of the complexes exhibited a molecular ion peak [M+] at m/z = 849.47 (**1**), m/z = 877.50 (**2**), m/z = 849.47 (**3**), m/z = 876.49 (**4**), m/z=1073.72 (**5**), which is indicative of the monomeric nature of these complexes with two ligands coordinated to the cobalt center.

In the ^{1}H NMR spectrum of complex **1**, the broad signal corresponding to –OH phenol protons was not detected, indicating the deprotonation of these groups. Moreover, a shift of the signal corresponding to the imine group CH=N, which appeared at δ 8.82 ppm for the ligand **L1** and at 8.95 ppm for the complex **1** indicated the coordination of the ligand in a tridentate manner via the formation of a Co-N and two Co-O bonds.

This coordination mode was confirmed by X-ray diffraction of crystals of complex **5** obtained by vapor diffusion from CH_2Cl_2 in Et_2O at room temperature. The molecular structure of this complex is depicted in Figure 4, and a selection of bond distances and angles is reported in Table 1.

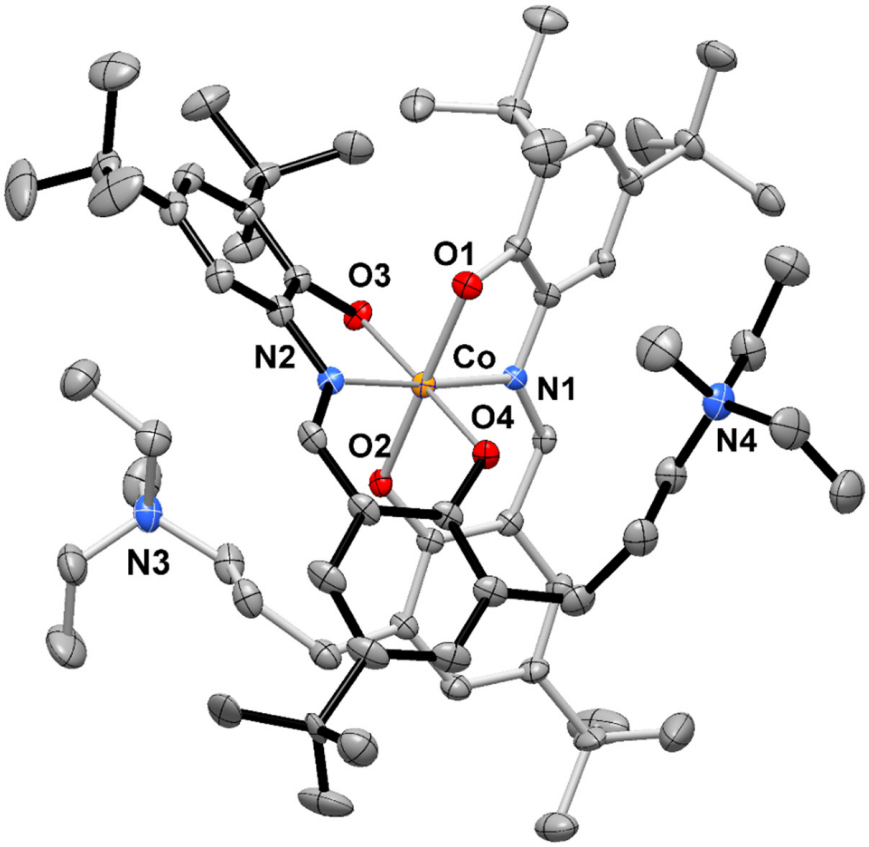

Figure 4. Molecular structure of the cationic Co(III) complex **5**. (Ortep drawing with displacement ellipsoids at 50% probability level. H atoms not shown for clarity).

The crystallographic independent unit contains a cationic metal complex counterbalanced by a I_3^- anion. The cobalt atom exhibits a distorted octahedral geometry formed by two meridionally coordinated ligands which behave as tridentate through the phenoxo oxygen atoms and the imino nitrogen. The Co-N bond distances are of 1.893(3) and 1.887(3) Å, and the Co-O ones vary in between 1.890(2)–1.906(2) Å. These values are within the range previously reported for Co(III) complexes bearing tridentate ligands [33,34].

2.2.2. Preparation and Characterization of Mn(II)(ONONu) Complexes

The manganese (II) complexes (**7**–**8**) bearing ONONu ligands were prepared by reacting the tetrahydrated $Mn(OAc)_2$ precursor with the previously synthetized cationic ligands (**L1**–**I** or **L2**–**I**) in dry ethanol, as depicted in Scheme 3.

Table 1. Distances (Å) and angles (°) of the compound **5**.

Co-N(1)	1.893(3)	Co-O(2)	1.890(2)
Co-N(2)	1.887(3)	Co-O(3)	1.906(2)
Co-O(1)	1.903(2)	Co-O(4)	1.904(2)
N(1)-Co-N(2)	174.35(12)	N(2)-Co-O(4)	92.83(12)
N(1)-Co-O(1)	85.71(11)	O(1)-Co-O(2)	179.01(10)
N(1)-Co-O(2)	93.38(11)	O(1)-Co-O(3)	87.82(11)
N(1)-Co-O(3)	90.61(11)	O(1)-Co-O(4)	92.30(11)
N(1)-Co-O(4)	91.35(11)	O(2)-Co-O(3)	91.78(11)
N(2)-Co-O(1)	90.32(12)	O(2)-Co-O(4)	88.12(11)
N(2)-Co-O(2)	90.56(11)	O(3)-Co-O(4)	178.05(10)
N(2)-Co-O(3)	85.22(12)		

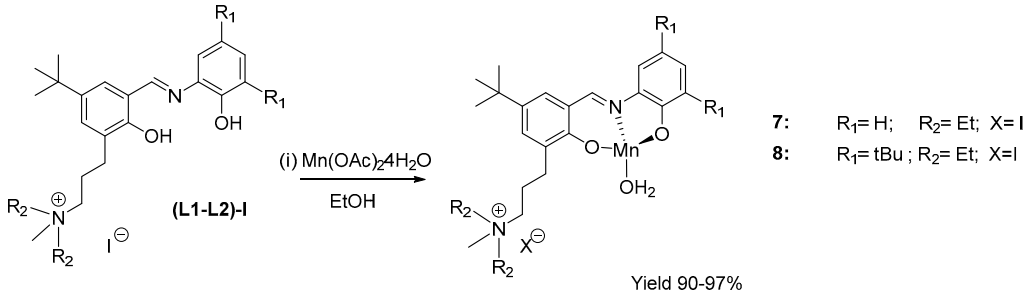

Scheme 3. Synthesis of Mn(II)(ONONu) complexes (**7**–**8**).

These manganese compounds were isolated as brown and air-stable solids and characterized by mass spectroscopy (ESI-TOF), FTIR spectroscopic techniques, UV-visible and magnetic susceptibility.

Mass spectra of the complexes exhibited a molecular ion peak [M^+] at m/z = 468.2 (**7**) and m/z = 579.4 (**8**), which was indicative of the monomeric nature of these complexes with one ligand coordinated to the Mn center.

In order to clarify the binding mode of ONONu ligands to the metal center, FTIR spectra of the metal complexes were recorded and compared with those of the corresponding ligands. The most representative frequencies are summarized in Table 2. The synthesized Mn(II) complexes showed a weak broad absorption band in the range 3370–3440 cm^{-1}, which was assigned to ν (OH_2) of the coordinated water molecule associated with the complexes, as previously described [35,36]. Furthermore, a narrow intense band in the region 830–840 cm^{-1}, specific for the coordinated water molecule, confirms the coordination of an aquo ligand to the metal center (Mn-OH_2) [35]. These absorption bands are not present in the free ligands, which conversely show the characteristic O-H stretching band frequency displaced around 2950 cm^{-1} [37–39]. The expected intramolecular hydrogen bridge OH···N=C band in the free ligand in the range of 3300–3800 cm^{-1} was not detected. In fact, hydrogen bonds in Schiff base ligands are very strong and as stronger the H-bond is, the bandwidth increases, then this band is sometimes not detected [40]. The participation of the OH group is apparent from the shift in position of the δ (OH) in-plane bending at 1477 cm^{-1}, while in the free ligand appears at 1456 cm^{-1}. The strong band around 1617 cm^{-1}, characteristic of ν(C=N) in the free ligand, was shifted to lower frequency region (1539 cm^{-1}) upon coordination of the Schiff base ligand to metal salts. Likewise, the phenolic band corresponding to the ν(C-O) in the ligands shifted upward by 50 cm^{-1} from 1220 cm^{-1}, supporting the coordination of phenolic oxygen to the metal center. This signal has decreased, demonstrating the involvement of the phenolic oxygen atom in the coordination [41]. Finally, evidence of the bonding of the Schiff base ligands to manganese

(II) was evidenced in the spectra of the complexes by the appearance of new bands in the region 600–400 cm^{-1} due to ν(Mn-O) and ν(Mn-N) stretching vibrations [36,42].

Table 2. FTIR spectral frequencies for the manganese (II) complexes and novel ONONu ligands.

Comp.	ν (OH_2)	ν (OH)	ν (C=N)	δ(OH) in Plane Bending	ν (C-O)	ν (Mn-OH_2)	ν (Mn-O)	ν (Mn-N)
L1	—	2953 (s)	1617 (s)	1456 (s)	1220 (m)	—	—	—
7	3372 (br)	2955 (s)	1539 (s)	1477 (m)	1269 (m)	835	603 (w)	539 (w)
L2	—	2953 (s)	1615 (m)	1460 (s)	1265 (m)	—	—	—
8	3414 (br)	2952 (s)	1538 (m)	1444 (s)	1265 (s)	832	576 (w)	545 (w)

The electronic spectra of the ligands and the complexes were obtained in 10^{-3} M solutions in CH_2Cl_2 at room temperature and recorded in the range of 190–720 nm. The absorption bands in the electronic spectra of the free ligands appear in the UV-Vis region (200–400 nm) and exhibit three bands due to the π→π* and n→π* transitions. The bands at λ_{max} 364 nm in the case of ligand **L1** and λ_{max} 374 nm for **L2** were assigned to n→π* transitions in the ligands. The transitions π→π* were observed at λ_{max} 278 nm and 238 nm (**L1**) and λ_{max} 277 nm and 237 nm (**L2**). The spectra of the Mn(II) complexes show slight variations in the position and intensity of these bands, which can be assigned to intraligand transitions modified by complexations. The bands corresponding to π→π* transitions appear at 297 nm and 234 nm in the case of complex **7**, and λ_{max} 294 and 238 nm for compound **8**. Moreover, the spectra of the Mn(II) complexes exhibit new weak absorption bands in the visible region, confirming the coordination. These spin forbidden d-d transition bands are observed as broad shoulder bands with low intensity and not well defined. In the case of complex **7,** this absorption band appears at λ_{max} 452 nm, while for complex **8**, this band was detected at λ_{max} 339 nm.

Further characterization of these manganese complexes was carried out through magnetic susceptibility measurements. Previous results with ONO ligands coordinated to manganese (II) exhibited a μ_{eff} value of 5.21 BM (Mn^{2+}), value in concordance with a tetrahedral structure [35]. The manganese complexes **7**–**8** revealed a μ_{eff} = 5.94 BM, in agreement with values in the literature for other Mn(II) compounds [42–44].

2.3. Catalytic Activity of the M(ONONu)X Complexes in the Carbon Dioxide/Epoxide Coupling Reactions

Catalytic cycloaddition reactions of propylene oxide with CO_2 to form propylene carbonate were carried out to evaluate the catalytic activity of the new Co and Mn complexes. These reactions were carried out in neat propylene oxide without any co-catalyst.

The catalytic results obtained using cobalt complexes (Scheme 2) and manganese complexes (Scheme 3) are presented in Tables 3 and 4, respectively.

All the catalytic reactions were carried out at 30 bars for 16 h using a 0.02 mol% of catalyst and the only product obtained in all the reactions with cobalt catalysts was propylene carbonate (PC, see crude NMR in Figure S1, Supplementary Materials). Cobalt catalyst containing iodide as counterion (**1** and **4**–**6**) were first tested at 80 °C (entries 1, 5, 6 and 8) to afford 13, 5, 26 and 20% of yield, respectively. When the temperature was raised to 120 °C using the same catalysts (entries 2, 7 and 9) the yields increased to 33–37%. All these catalysts showed a similar behavior.

The effect of the counterion has been studied for **L1** (entries 1–4). At the same temperature, the iodide affords the same yield. When nitrate is the counterion, the catalyst is not active at 80 °C and at 120 °C exhibits a very low yield (entry 4). Under the same catalytic conditions complexes **2** and **4**–**6** were also tested, showing similar results.

Table 3. Catalytic coupling reactions of propylene oxide and CO_2 with Co(ONONu) complexes [a].

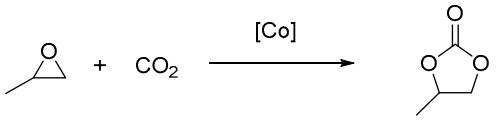

Entry	Cat	Ligand	T(°C)	% Isolated Yield	TON	TOF (h^{-1})
1	**1**	**L1-I**	80	13	661	41
2	**1**	**L1-I**	120	35	1758	109
3	**2**	**L1-Br**	80	12	600	38
4	**3**	**L1-NO_3**	120	7	368	23
5	**4**	**L4-I**	80	5	250	16
6	**5**	**L2-I**	80	26	1294	81
7	**5**	**L2-I**	120	33	1650	116
8	**6**	**L3-I**	80	20	1011	63
9	**6**	**L3-I**	120	37	1850	103

[a] Typical reaction conditions: P = 30 bar CO_2, t = 16 h, 0.02 mol% of catalyst.

Table 4. Catalytic coupling reactions of propylene oxide and CO_2 with Mn(ONONu) complexes.

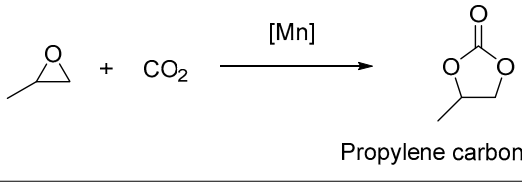

Entry	Cat	Mol%	T(°C)	P(bar)	t(h)	% Isolated Yield	TON	TOF (h^{-1})
1	**7**	0.05	80	30	16	89	1780	111
2	**7**	0.01	80	10	16	31	3092	193
3	**7**	0.01	120	30	0.5	9	905	1810
4	**8**	0.01	80	30	16	17	1714	107
5	**8**	0.01	120	30	16	48	4860	304

The presence of two *tert*-butyl groups (complexes **5** and **6**) provided a robust catalyst with high productivity when the reaction was carried out at 80 °C (Table 3, entries 6 and 8). With the same catalyst **5**, a TOF of 116 h^{-1} was obtained at 120 °C, which is a remarkable result for a cobalt catalyst (Table 3, entry 7).

As has been mentioned in the literature, there are few examples of manganese complexes that have been tested in this reaction [13,19–21,45,46]. Among these, only in some cases, the manganese complexes have been used as catalysts in the selective formation of cyclic carbonates from epoxides and CO_2 under neat conditions and without any co-catalysts [20,45]. Herein, we decided to test **L1** and **L2** with a Mn complex to determine their activity as novel catalysts. By varying the ratio catalysts/substrate, the temperature and the pressure of CO_2, the best result was obtained for the catalyst Mn(ONOEt)I (**7**) and was obtained using the mildest reaction conditions (80 °C, 10 bar and 0.01 mol% catalyst, Table 4, entry 2), achieving a TON of 3092. This catalyst was tested under similar conditions and provided a TOF value of 1810 h^{-1}. To the best of our knowledge, this is the best result obtained to date using manganese catalysts in this reaction. The introduction of two *tert*-butyl groups in the structure of the ligand (complex **8**) also improved the catalytic performance, providing a TON of 4860. Results obtained in this work show that the catalytic activity of the cobalt complexes was observed generally lower than that of the analogous manganese catalysts, which are 2.5 times more active than cobalt ones. However, when the reaction was carried out at 80 °C, the results were quite similar (entry 6 in Table 2 vs. entry 4 in Table 3). The enhanced activity of the manganese catalysts demonstrated that these complexes were more robust than cobalt ones.

In terms of mechanism, the cycloaddition of CO_2 to epoxides takes place in a two-step process. With the catalyst reported here, in the first instance, the decoordination or partial decoordination of one of the ligands (Scheme 4) must take place to generate a vacant coordination site. Then, when the epoxide coordinates to the metal center, the nucleophilic attack from the counter-ion of the ligand can open the epoxide, forming an alkoxide which is positively charged.

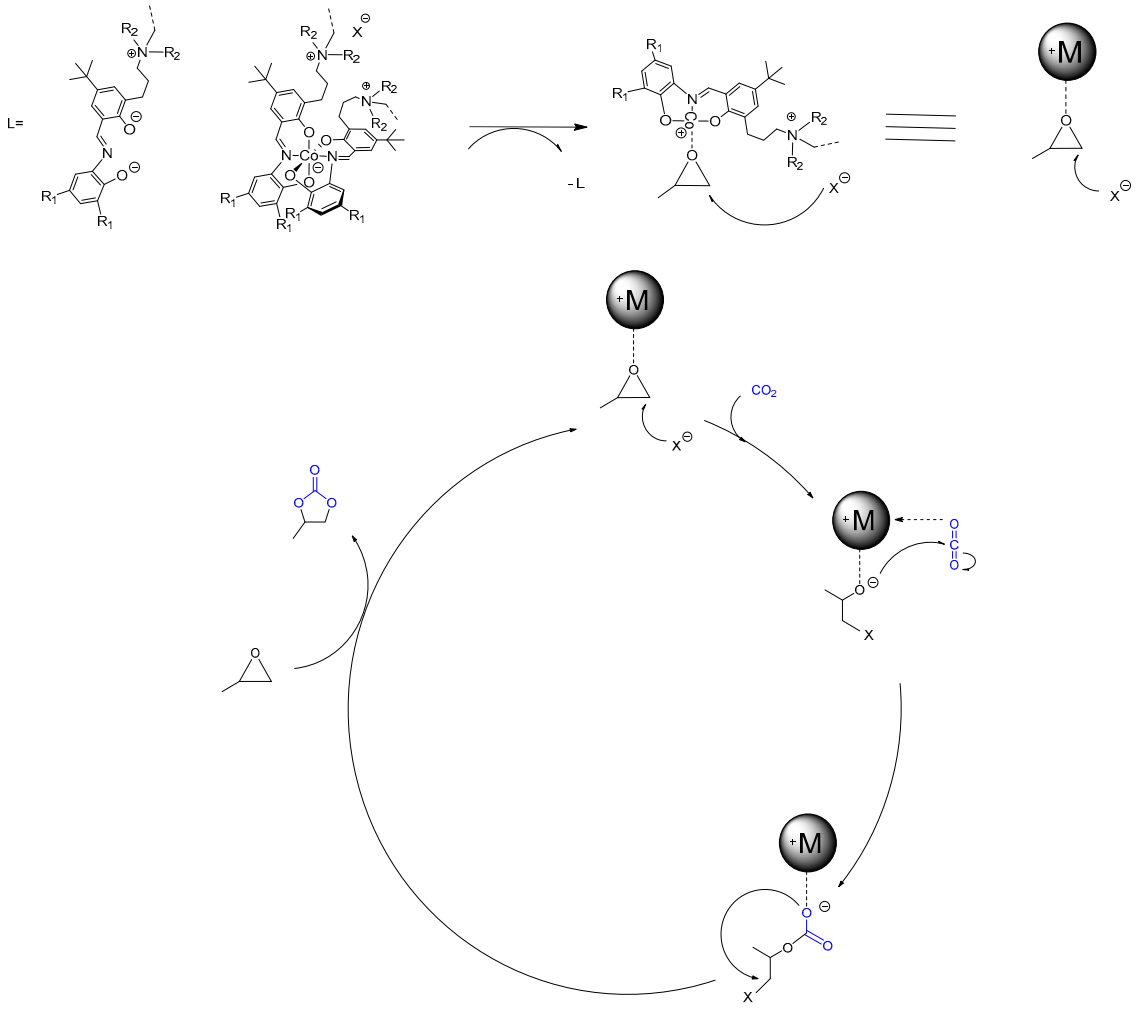

Scheme 4. Activation of the catalysts and proposed mechanism for catalytic coupling reaction of propylene oxide and CO_2 to form propylene carbonate.

At this point, the insertion of CO_2 into a metal alkoxide is followed by the insertion of epoxide into a metal-carboxylate species. In a last step, the intramolecular nucleophilic attack of the alkoxide leads to the formation of cyclic carbonate (Scheme 4), and the cycle is repeated several times to afford the desired product.

This process is known to be favored by temperature and the nucleophilicity of the counterion of the ligand, which acts as an initiator in the reaction mechanism by promoting the opening of the propylene oxide.

3. Materials and Methods

3.1. General Procedures

All reactions and manipulations were carried out under inert atmosphere using conventional Schlenk techniques. The chemicals *o*-aminophenol (CAS nº. 95-55-6) and iodomethane (CAS nº. 74-88-4) were of reagent grade, obtained from commercial sources such as Sigma-Aldrich (Spain), Alfa Aesar (Spain) or TCI (Europe) and used without further

purification. Solvents were purified by using a Braun MB SPS-800 system and stored under N_2. Propylene oxide, absolute ethanol and methanol used in the reactions were dried over CaH_2 and deoxygenated before their use. An oxygen/moisture trap (Agilent) was used in the line of CO_2 (SCF Grade, 99.999%, Air Products, Spain). Cobalt (II) acetate tetrahydrate was purchased from Aldrich (CAS nº. 6147-53-1). Ligand (**L1**) was synthesized according to our former study/ literature methods [21]. Fragments (**F1**) and (**F2**) were obtained as previously described by Lu and coworkers in the literature [32].

3.2. General Analysis and Methods

Solution NMR spectra (^{1}H and ^{13}C NMR spectra) were obtained at the "Servei de Recursos Científics i Tècnics (SRCiT)" of the University Rovira and Virgili (URV) using a 400 MHz Varian Mercury VX400 spectrometer and calibrated to the residual solvent peaks. IR spectra were recorded on a Midac Grams/386 spectrometer in ATR or KBr in the range of 4000–400 cm^{-1}. Mass spectra were recorded using an Agilent 1100 MSD at Universitat Jaume I. HR-MS (ESI-TOF) analyses were performed on an Agilent time-of-flight 6210 spectrometer at the SCRiT of the URV. Elemental analyses were performed at the "Serveis Científics d'Investigació Científica (SCIC)" of the University Jaume I. Electronic spectra were recorded in the 190–800 nm range using a Shimadzu MultSpec-1501 instrument. These spectra in CH_2Cl_2 solutions were obtained at room temperature using 1.0 cm quartz cells. Magnetic susceptibilities were measured on a Sherwood MSB mk1 magnetic susceptibility balance with KK105 calibration standard.

3.3. Preparation and Characterization of Ligands

3.3.1. General Procedure for Ligands **L1**–**L4**

A solution of salicylaldehyde (**F1**) (380 mg, 1.3 mmol) in dry ethanol (5 mL) was stirred at 80 °C and a solution of *o*-aminophenol (142 mg, 1.3 mmol) in dry ethanol (5 mL) was added dropwise during half an hour and subsequently refluxed for 3 h and an orange precipitate was formed. Once the reaction reached room temperature, the solvent was removed by filtration and the raw product was obtained as an orange solid. Through washing several times with ethanol and following drying under vacuum overnight, the pure product was obtained as an orange powder.

L1: Quantitative yield. RMN ^{1}H (δ, DMSO-d^6): 0.92 (t, J = 7.2 Hz, 6H, CH_3), 1.27 (s, 9H, ^{t}Bu), 1.68 (m, 2H, CH_2), 2.42 (m, 6H, CH_2), 2.60 (t, J = 7.3 Hz, 2H, CH_2), 6.83 (m, 1H, CH=), 6.95 (dd, J = 8.1 Hz, 1.2 Hz, 1H, CH=), 7.09 (m, 1H, CH=), 7.29 (d, J = 2.5 Hz, 1H, CH=), 7.33 (dd, J = 7.9, 1.4 Hz, 1H, CH=), 7.41 (d, J = 2.5 Hz, 1H, CH=), 8.77 (s, 1H, CH=N), 9.72 (*br* s, 1H, OH), 13.95 (*br* s, 1H, OH). RMN ^{13}C (δ, $CDCl_3$): 10.39 (CH_3CH_2), 26.16 (CH_2), 27.47 (CH_2), 31.43 (CH_{3tBu}), 34.05 (Cq_{tBu}), 46.10 (CH_2), 51.02 (CH_2), 115.60 (CH_{arom}), 116.62 (Cq), 117.76 (CH_{arom}), 120.47 (CH_{arom}), 125.58 (Cq), 128.29 (CH_{arom}), 129.11 (Cq), 131.72 (CH_{arom}), 135.93 (Cq), 141.74 (CH_{arom}), 150.67 (Cq-O), 156,95 (Cq-O), 161.83 (CH=N). Selected IR bands (KBr, cm^{-1}): 2953 (ν_{OH}), 1617 (C=N), 1456 (δ(OH), 1220 (ν_{C-O}), 745 (ar C=C). UV-Vis spectrum in CH_2Cl_2 [λ_{max} (nm), ε(dm^3 cm^{-1} mol^{-1})]: 238 (42017), 278 (35971), 364 (27472).

L2: Quantitative yield. RMN ^{1}H (δ, $CDCl_3$): 1.12 (t, J = 7.2 Hz, 6H, CH_3), 1.33 (s, 9H, *t*Bu), 1.34 (s, 9H, *t*Bu), 1.45 (s, 9H, *t*Bu), 1.92 (m, 2H, CH_2), 2.62 (m, 2H, CH_2), 2.74–2.68 (m, 6H, 3xNCH_2), 7.05 (d, J = 2.3 Hz, 1H, CH_{arom}), 7.25 (d, J = 2.3 Hz, 1H, CH_{arom})7.31 (d, J = 2.5 Hz, 1H, CH_{arom}), 7.46 (d, J = 2.3 Hz, 1H, CH_{arom}), 8.82 (s, 1H, CH=N), 9.6 (*br* s, 1H, OH), 13.7 (br s, 1H, OH). RMN ^{13}C (δ, $CDCl_3$): 10.35 (CH_3CH_2), 26.02 (-CH_2-), 27.53 (NCH_2), 29.48 (CH_{3tBu}), 31.45 (CH_{3tBu}), 31.63 (CH_{3tBu}), 34.07 (Cq_{tBu}), 34.58 (Cq_{tBu}), 35.00 (Cq_{tBu}), 46.16 (NCH_2), 51.05 (CH_2), 112.18 (CH_{arom}), 119.60 (Cq), 122.80 (CH_{arom}), 125.78 (CH_{arom}), 128.88 (Cq), 131.44 (CH_{arom}), 135.33 (Cq), 135.80 (Cq), 141.95 (Cq), 142.11 (Cq), 146.64 (Cq-O), 156,23 (Cq-O), 161.98 (CH=N). Selected IR bands (KBr, cm^{-1}): 2953 (ν_{OH}), 1617 (C=N), 1456 (δ(OH), 1220 (ν_{C-O}), 745 (ar C=C). UV-Vis spectrum in CH_2Cl_2 [λ_{max} (nm), ε(dm^3 cm^{-1} mol^{-1})]: 235.0 (42553), 296 (33784), 339 (29498).

L3: Quantitative yield. RMN ^{1}H (δ, DMSO-d^6): 0.85 (t, J = 7.23 Hz, 6H, CH_3), 1.04 (t, J = 7.0 Hz, 2H, -CH_2-), 1.20-1.25 (m, 4H, CH_2), 1.28 (2 s, 18H, *t*Bu), 1.30-1.35 (m, 4H, CH_2), 1.38 (s, 9H, *t*Bu), 1.7 (m, 2H, CH_2), 2.36 (m, 4H, NCH_2), 2.61 (m, 2H, NCH_2), 7.06 (s, 1H, CH=), 7.07 (s, 1H, CH=), 7.12 (s, 1H, CH=), 7.51 (s, 1H, CH=), 8.5 (*br* s, 1H, OH), 8.82 (s, 1H, CH=N). RMN ^{13}C (δ, $CDCl_3$): 14.09 (CH_{3Bu}), 20.77 (-CH_2-$_{Bu}$), 27.42 (NCH_2-$_{Bu}$), 29.49 ($CH_{3\ tBu}$), 29.82 (Cq_{tBu}), 31.47 ($CH_{3\ tBu}$), 31.61 (Cq_{tBu}), 31.65 ($CH_{3\ tBu}$), 34.07 (CH_2), 34.58 (CH_2), 35.00 (CH_2), 52.58 (NCH_2), 53.07 (NCH_2), 112.06 (CH_{arom}), 122.76 (CH_{arom}), 125.58 (CH_{arom}), 131.49 (CH_{arom}), 135.78 (Cq), 141.87(Cq), 142.06 (Cq), 146.71 (Cq), 156.29(Cq), 161.81 (CH=N). Selected IR bands (KBr, cm^{-1}): 2953 (ν_{OH}), 1615 (C=N), 1460 (δ(OH), 1224 (ν_{C-O}), 765 (ar C=C). UV-Vis spectrum in CH_2Cl_2 [λ_{max} (nm), ε(dm^3 cm^{-1} mol^{-1})]: 237 (42194), 277 (36101), 374 (26738).

L4: Quantitative yield. RMN ^{1}H (δ, DMSO-d^6): 1.09 (t, J = 7.2 Hz, 6H, CH_3), 1.33 (s, 9H, *t*Bu), 1.9 (m, 2H, CH_2), 2.29 (s, 3H, CH_3), 2.32 (s, 3H, CH_3), 2.58 (m, 2H, NCH_2), 2.73–2.64 (m, 6H; 2× NCH_2, 1-CH_2-), 6.89-6.84 (m, 2H, CH_{arom}), 7.30 (d, J = 2.5 Hz, 1H, CH_{arom}), 7.43 (d, J = 2.3 Hz, 1H, CH_{arom}), 8.81 (s, 1H, CH=N), broad signals corresponding to OH not observed in this solvent. RMN ^{13}C (δ, $CDCl_3$): 10.60 (CH_3CH_2), 15.78 (CH_3), 20.69 (CH_3), 26.23 (-CH_2-), 27.54 (NCH_2), 31.45 (CH_{3tBu}), 34.07 (Cq_{tBu}), 46.22 (NCH_2), 51.23 (CH_2), 115.59 (CH_{arom}), 119.45 (Cq), 124.48 (Cq), 125.65 (Cq), 129.11 (CH_{arom}), 130.26 (Cq), 131.42 (CH_{arom}), 135.33 (Cq), 135.39 (Cq), 141.95 (Cq), 141.80 (Cq), 146.43 (Cq-O), 156,46 (Cq-O), 161.85 (CH=N). Selected IR bands (KBr, cm^{-1}): 2954 (ν_{OH}), 1616 (C=N), 1462 (δ(OH), 1224 (ν_{C-O}), 750 (ar C=C).

3.3.2. General Procedure for Quaternization of the Ligands (Example for ligand **L1-I**)

L1 is dissolved in dichloromethane and excess amount of CH_3I was added and the resulting solution was stirred at room temperature for 3 h. Finally, the solvent was evaporated under reduced pressure. The pure product was obtained in a quantitative yield.

L1-I: Quantitative yield. RMN ^{1}H (δ, DMSO-d^6): 1.16 (t, J = 7.2 Hz, 6H, CH_3), 1.29 (s, 9H, ^{t}Bu), 1.94 (m, 2H, CH_2), 2.65 (m, 2H, CH_2), 2.90 (s, 3H, CH_3), 3.27 (m, 6H, CH_2), 6.86 (t, J = 7.6 Hz, 1H, CH=), 6.95 (m, 1H, CH=), 7.09 (m, 1H, CH=), 7.37 (m, 2H, CH=), 7.47 (d, J = 2.4 Hz, 1H, CH=), 8.98 (s, 1H, CH=N), 9.76 (*br* s, 1H, OH), 14.23 (*br* s, 1H, OH).

L1-Br: In this case, the quaternization was done using bromoethane as alkyl halide. Quantitative yield. RMN ^{1}H (δ, DMSO-d^6): 1.15 (t, J = 7.2 Hz, 6H, CH_3), 1.30 (s, 9H, ^{t}Bu), 1.96 (m, 2H, CH_2), 2.67 (m, 2H, CH_2), 3.10 (t, 3H, CH_3), 3.25 (m, 6H, CH_2), 3,98 (m, 2H, CH_2), 6.88 (t, J = 7.6 Hz, 1H, CH=), 6.94 (m, 1H, CH=), 7.10 (m, 1H, CH=), 7.39 (m, 2H, CH=), 7.50 (d, J = 2.4 Hz, 1H, CH=), 8.96 (s, 1H, CH=N), 9.56 (*br* s, 1H, OH), 14.13 (*br* s, 1H, OH).

3.4. Preparation and Characterization of Cobalt and Manganese Complexes

3.4.1. General procedure and Characterization of the Compounds [Co(ONONu)$_2$(S)](Example for Ligand **L1-I**)

Firstly, the ligands were quaternized following the procedure mentioned above and used without further purification for the reaction with cobalt precursor as follows:

A solution of the ligand (**L1-I**) (72 mg; 0.138 mmol) in methanol (5 mL) was added dropwise to a suspension of hydrated cobalt acetate (II) (35 mg; 1.4 equiv.) in methanol (15 mL). After stirring the reaction during 3 h at room temperature the mixture was stirred under air atmosphere and left overnight. The initial orange solution changed to red–brown. The solvent was evaporated under reduced pressure and the solid was washed with hexane and dried under vacuum overnight.

1: Yield 43% (65 mg). RMN ^{1}H (δ, DMSO-d^6): 0.87 (t, J = 6.6 Hz, 12H, CH_3), 1.24 (s, 18H, ^{t}Bu), 2.01 (m, 4H, CH_2), 2.21 (m, 4H, CH_2), 2.34 (s 6H, CH_3), 2.72 (m, 12H, CH_2), 6.38 (d, J = 8.0 Hz, 2H, CH=), 6.46 (t, J = 7.1 Hz, 2H, CH=), 6.77 (t, J = 7.7 Hz, 2H, CH=), 6.89 (s, 2H, CH=), 7.45 (s, 2H, CH=), 8.16 (d, J = 7.5 Hz, 1H, CH=), 8.95 (s, 1H, CH=N). FTIR (ATR, cm^{-1}): 2951 (NR_4+), 1715, 1611 (C=N), 1579, 1534, 1479, 1455, 1426, 1384, 1300, 1265, 1226, 1027, 750, 529. ESI-TOF (m/z): 849.4723 $[M]^+$.

2: Yield 45%. RMN ^{1}H (δ, DMSO-*d*^{6}): 0.86 (m, 18H, CH_3), 1.24 (s, 18H, *t*Bu), 1.87 (m, 2H, CH_2), 2.21 (m, 2H, CH_2), 2.48 (m, 12H, NCH_2), 2.62 (m, 8H, CH_2), 6.39 (m, 2H, CH=), 6.47 (m, 2H, CH=), 6.78 (m, 2H, CH=), 6.91 (s, 2H, CH=), 7.45 (s, 2H, CH=), 8.15 (m, 2H, CH=), 8.97 (s, 2H, CH=N). RMN ^{13}C (δ, DMSO-*d*^{6}): 6.51 (NCH_2CH_3), 8.29 (NCH_2CH_3), 27.92 (C_q-*t*Bu), 30.47 (CH_2), 30.53 (CH_3-*t*Bu), 33.08 (CH_2), 49.38 (CH_2-N), 51.73 (CH_2-N), 111.92 (CH_{arom}), 114.70 (CH_{arom}), 117.61 (C_q), 118.85 (C_q), 122.29 (CH_{arom}), 127.05 (CH_{arom}), 129.31 (CH_{arom}), 131.03 (CH_{arom}), 133.76 (C_q), 141.05 (C_q-N), 151.40 (C_q-O), 161.63 (C_q-O), 168.63 (CH=N). ESI-TOF (*m*/*z*): 877.5041 [M]$^{+}$.

3: Yield 48%. Once the complex **1** was obtained, an equivalent of $AgNO_3$ was added to change the counterion. RMN ^{1}H (δ, DMSO-*d*^{6}): 0.88 (t, *J* = 6.6 Hz, 12H, CH_3), 1.25 (s, 18H, *t*Bu), 2.35 (m, 6H, CH_3), 2.72 (m, 12H, CH_2), 4.09 (m, 8H, CH_2), 6.39 (d, *J* = 8.0 Hz, 2H, CH=), 6.47 (t, *J* = 7.1 Hz, 2H, CH=), 6.78 (t, *J* = 7.7 Hz, 2H, CH=), 6.90 (s, 2H, CH=), 7.45 (s, 2H, CH=), 8.16 (d, *J* = 7.5 Hz, 2H, CH=), 8.96 (s, 2H, CH = N). ESI-TOF (*m*/*z*): 849.4723 [M]$^{+}$.

4: Yield 54%. RMN ^{1}H (δ, DMSO-*d*^{6}): 0.77 (t, 12H, CH_3), 1.0-1.1 (m, 4H CH_2), 1.24 (s, 18H, *t*Bu), 1.77 (m, 6H, CH_3), 2.0 (m, 8H, CH_2), 2.25 (s, 3H, CH_3), 2.32 (s, 3H, CH_3), 2.73 (m, 8H, CH_2), 6.5 (m,1H, CH_{arom}), 6.7 (m, 1H, CH_{arom}), 7.3 (s, 1H, CH_{arom}), 7.8 (m, 1H, CH_{arom}), 8.7 (s, 1H, CH=N). RMN ^{13}C (δ, DMSO-*d*^{6}): 11.34 (NCH_2CH_3), 17.10 (CH_3), 20.92 (CH_3), 25.18 (C_q-*t*Bu), 29.53 (CH_2), 31.94 (CH_3-*t*Bu), 33.08 (C_q), 46.33 (CH_2), 51.14 (C_q), 113.11 (CH_{arom}), 119.15 (C_q), 119.76 (C_q), 125.69 (C_q), 128.10 (CH_{arom}), 129.25 (CH_{arom}), 130.03 (CH_{arom}), 132.76 (C_q), 133.56 (C_q), 140.05 (C_q-N), 151.16 (CH=N), 162.55 (C_q-O), 166.19 (C_q-O). ESI-TOF (*m*/*z*): 876.49 [M]$^{+}$

5: Yield 55%. RMN ^{1}H (δ, DMSO-*d*^{6}): 0.86 (s, 12H, NCH_2CH_3), 0.90 (s, 18H, *t*Bu), 1.19-1.38 (m, 4H, CH_2), 1.25 (s, 18H, *t*Bu), 1.35 (s, 18H, *t*Bu), 2.02-2.21 (m, 4H, CH_2), 2.36 (s, 6H, NCH_3), 2.61-2.86 (m, 12H, CH_2), 6.72 (broad s, 2H, CH_{arom}), 6.83 (broad s, 2H, CH_{arom}), 7.48 (broad s, 2H, CH_{arom}), 7.97 (broad s, 2H, CH_{arom}), 8.91 (s, 2H, CH=N). RMN ^{13}C (δ, DMSO-*d*^{6}): 8.04 (NCH_2CH_3), 21.99 (CH_2), 29.54 (*t*Bu), 29.87 (CH_2), 32.03 (*t*Bu), 32.57 (*t*Bu), 33.71 (C_q *t*Bu), 34.43 (C_q *t*Bu), 35.01 (C_q *t*Bu), 46.50 (NCH_3), 55.20 ($NCH_2CH_2CH_2$), 55.49 ($NCH_2CH_2CH_2$), 59.50 (NCH_2CH_3), 109.58 (CH_{arom}), 119.58 (C_q), 120.60 (CH_{arom}), 129.37 (CH_{arom}), 129.16 (CH_{arom}), 133.31 (C_q), 132.87 (C_q), 131.67 (C_q), 137.56 (C_q), 140.83 (NC_q), 150.68 (CH=N), 162.27 (C_q-O), 166.98 (C_q-O). ESI-TOF (*m*/*z*) =1073.72 [M]$^{+}$.

6: Yield 46%. RMN ^{1}H (δ, DMSO-*d*^{6}): 0.85 (m, 12H, CH_3), 1.5-1.7 (s, 54H, *t*Bu), 2.02 (m, 12H, CH2), 2.21 (s, 6H, CH_3), 2.80 (m, 24H, CH_2), 6.72 (broads, 2H, CH=), 6.85 (broad s, 2H, CH=), 7.47 (broads, 2H, CH=), 8.00 (broad s, 2H, CH=), 8.93 (s, 2H, CH=N).

3.4.2. Synthesis and Characterization of the Compounds [Mn(ONONu)] (**7**–**8**)

A suspension of ligand (**L1-I**) (69 mg; 0.131 mmol) in dry ethanol (10 mL) was added dropwise to a refluxed solution of hydrated magnesium acetate (57 mg; 0.24 mmol) in dry ethanol (5 mL). In a few minutes, the warmed solution changed from pink to pale brown and finally with formation of a yellow precipitate. When the addition of the ligand was completed, the dark brown mixture obtained was heated to reflux during 2 h under nitrogen atmosphere. Finally, the mixture was refluxed and stirred overnight in air atmosphere. After cooling to room temperature, the solid product was collected by filtration, washed with hexane, and dried under vacuum overnight.

7: Yield 97%. Elemental analysis for $C_{25}H_{37}MnN_2O_3I{\cdot}H_2O$: 4.57 %N, 48,95 %C, 6.41 %H. Found: 4.64 %N, 47.25 %C, 5.85 %H. ESI (+)(DCM/MeOH) (m/z): 468.2 [M]$^{+}$, 481.2 [M+CH_3OH)]$^{+}$. Magnetic susceptibility μ_{eff} (298 k)= 5.94 BM (Mn^{2+}) at room temperature. Selected FT-IR bands (KBr, cm^{-1}): 2954 (ν_{OH}), 1538 (C=N), 1580, 1539, 1475, 1445, 1384, 1264, 1029, 930, 831, 750, 645. UV-Vis spectrum in CH_2Cl_2 [λ_{max} (nm), ε(dm^3 cm^{-1} mol^{-1})]: 234 (42735), 297 (33670), 452 (22124).

8: Yield 90%. Elemental analysis for $C_{33}H_{53}MnN_2O_3I$: 3.96 %N, 56.01 %C, 7.55 %H. Found: 3.94 %N, 56.98 %C, 8.13 %H. ESI (+) (DCM/MeOH) (m/z): 579.4 [M-H]$^{+}$. Selected FT-IR bands (KBr, cm^{-1}): 2952 (ν_{OH}), 1538 (C=N), 1444, 1362, 761 (Mn-OH_2), 557,

427. UV-Vis spectrum in CH_2Cl_2 [λ_{max} (nm), ε(dm^3 cm^{-1} mol^{-1})]: 231 (43290), 296 (33783), 339 (29498).

3.5. X-ray Structure Determination

Data collection of the Co(III) complex **5** was performed at the X-ray diffraction beamline (XRD1) of the Elettra Synchrotron of Trieste (Italy), with a Pilatus 2M image plate detector. Complete dataset was collected at 100 K (nitrogen stream supplied by an Oxford Cryostream 700) with a monochromatic wavelength of 0.7000 Å through the rotating crystal method. The crystal was dipped in N-paratone and mounted on the goniometer head with a nylon loop. The diffraction data were indexed, integrated, and scaled using XDS [47]. The structure was solved by direct methods using SIR2014 [48]. Fourier analysis and refinement with the full-matrix least-squares method based on F^2 were performed with SHELXL-2019/2 [49]. Anisotropic thermal parameters were applied to all non-H atoms expect to a residual assigned as an oxygen water molecule at half occupancy. Hydrogen atoms were placed at calculated positions. A *tert*-butyl group was found disordered over two positions with refined occupancies 0.46/0.54(2). All the calculations were performed using the WinGX System, Ver 2018.3 [50].

Crystal Data and Details of Refinement

$C_{66}H_{103}CoI_3N_4O_{4.50}$, MW = 1464.15, triclinic system, space group $p\ -1$, a = 15.118(5), b = 16.790(5), c = 17.788(5) Å, α = 112.509(5), β = 114.004(5), γ = 93.607(5)°, V = 3680.3(19) $Å^3$, Z = 2, Dc = 1.321 g/cm^3, μ(Mo-Kα) = 1.535 mm^{-1}, F(000) = 1498, θ range = 1.36–28.75°. Final R1 = 0.0631, wR2 = 0.1866, S = 1.051 for 747 parameters and 18246 independent reflections of which 14190 with $I > 2\sigma(I)$; max positive and negative peaks in ΔF map = 1.693, −2.968 e. $Å^{-3}$.

3.6. Autoclave Experiments

The copolymerization tests were carried out in a 100 mL Berghof reactor. The reactors were introduced in a glovebox prior to use after 12 h over vacuum and the batch reactor was filled with the catalyst and PO in desired ratio. The reactor was sealed and outside of the glovebox was filled with CO_2 at the previous selected pressure and heated to the desired temperature. When the reaction time was reached, the reactor was cooled down in an ice bath and subsequently CO_2 was released slowly. Then, a sample of crude reaction mixture was taken for ^{1}H NMR test in order to evaluate the selectivity of the reaction. The crude was filtered through a short silica plug using dichloromethane as solvent. The solvent was evaporated over vacuum to recover cyclic carbonate until constant weight to determine the productivity and yield of the reaction (see ^{1}H NMR of purified PC in Figure S2, Supplementary Materials).

4. Conclusions

Novel homogeneous Co(III) and Mn(II) catalysts bearing a novel pendant-armed ONONu ligand, which includes a quaternary ammonium in the ligand structure, were synthesized. These catalysts are active in the reaction between CO_2 and propylene oxide to form cyclic carbonates and, to the best of our knowledge, the catalyst **8** exhibited the highest activity described for Mn systems (256 kg/(kg·h). This pendant arm of the structure acts as a co-catalyst and prevents the decomposition of the catalyst increasing its productivity and stability towards the formation of propylene carbonate.

Supplementary Materials: TThe following supporting information can be downloaded at: https://www.mdpi.com/article/10.3390/catal12111443/s1, (Figure S1: 1H NMR for the crude catalytic reaction of propylene oxide and CO_2 to obtain propylene carbonate; Figure S2: 1H NMR spectrum of the isolated propylene carbonate from the cycloaddition CO_2/propylene oxide product). CCDC 2205610 contains the supplementary crystallographic data for complex **5** in this paper. These data can be obtained free of charge from The Cambridge Crystallographic Data Centre via www.ccdc.cam.ac.uk/data_request/cif.

Author Contributions: M.V., B.K.M., C.G., S.C. and C.C. conceived and designed the experiments; M.V. and B.K.M. performed the experiments and methodology; M.V., B.K.M., C.G., S.C. and C.C. analyzed the data; C.G., E.Z., S.C. and C.C. contributed reagents/materials/analysis tools; M.D.B.G. and M.G.-R. found funding acquisition and project administration; M.V. and B.K.M. wrote and edited the paper; M.V., B.K.M., E.Z., C.G., S.C. and C.C. review the paper. All authors have read and agreed to the published version of the manuscript.

Funding: This research was funded by Repsol and CTQC (TQC16006S and TQC14029S) (now Eurecat). Spanish Ministerio de Economía y Competitividad for financial support AEI/FEDER UE (CTQ2016-75016-R) and the Catalan Departament d'Economia I Coneixement (2017 SGR 1472). Additionally, Instituto Valenciano de Competitividad Empresarial (IVACE) in the Comunitat Valenciana contributed within the context of CLIMA project (IMAMCA/2022/4) to this publication.

Conflicts of Interest: The authors declare no conflict of interest.

References

1. Hasan, M.M.F.; Rossi, L.M.; Debecker, D.P.; Leonard, K.C.; Li, Z.; Makhubela, B.C.E.; Zhao, C.; Kleij, A. Can CO_2 and Renewable Carbon Be Primary Resources for Sustainable Fuels and Chemicals? *ACS Sustain. Chem. Eng.* **2021**, *9*, 12427–12430. [CrossRef]
2. Zhang, Z.; Zheng, Y.; Qian, L.; Luo, D.; Dou, H.; Wen, G.; Yu, A.; Chen, Z. Emerging Trends in Sustainable CO_2-Management Materials. *Adv. Mater.* **2022**, *34*, 2201547. [CrossRef] [PubMed]
3. Parker, H.L.; Sherwood, J.; Hunt, A.J.; Clark, J.H. Cyclic Carbonates as Green Alternative Solvents for the Heck Reaction. *ACS Sustain. Chem. Eng.* **2014**, *2*, 1739–1742. [CrossRef]
4. Kamphuis, A.J.; Picchioni, F.; Pescarmona, P.P. CO_2-fixation into cyclic and polymeric carbonates: Principles and applications. *Green Chem.* **2019**, *21*, 406–448. [CrossRef]
5. Pescarmona, P.P. Cyclic carbonates synthesised from CO_2: Applications, challenges and recent research trends. *Curr. Opin. Green Sustain. Chem.* **2021**, *29*, 100457. [CrossRef]
6. Decortes, A.; Castilla, A.M.; Kleij, A.W. Salen-Complex-Mediated Formation of cyclic carbonates by cycloaddition of CO_2 to epoxides. *Angew. Chem. Int. Ed.* **2010**, *49*, 9822. [CrossRef]
7. Qin, Z.; Thomas, C.M.; Lee, S.; Coates, G.W. Cobalt-Based Complexes for the Copolymerization of Propylene Oxide and CO_2: Active and Selective Catalysts for Polycarbonate Synthesis. *Angew. Chem. Int. Ed.* **2003**, *42*, 5484. [CrossRef]
8. Whiteoak, C.J.; Kielland, N.; Laserna, V.; Escudero-Adán, E.C.; Martin, E.; Kleij, A.W. A powerful aluminum catalyst for the synthesis of highly functional organic carbonates. *J. Am. Chem. Soc.* **2013**, *135*, 1228. [CrossRef]
9. Tian, D.; Liu, B.; Gan, Q.; Li, H.; Darensbourg, D.J. Formation of Cyclic Carbonates from Carbon Dioxide and Epoxides Coupling Reactions Efficiently Catalyzed by Robust, Recyclable One-Component Aluminum-Salen Complexes. *ACS Catal.* **2012**, *2*, 2029–2035. [CrossRef]
10. North, M.; Pasquale, R. Mechanism of cyclic carbonate synthesis from epoxides and CO_2. *Angew. Chem. Int. Ed.* **2009**, *48*, 2946–2948. [CrossRef]
11. Mercadé, E.; Zangrando, E.; Claver, C.; Godard, C. Robust Zinc complexes that contain pyrrolidine-based ligands as recyclable catalysts for the synthesis of cyclic carbonates from carbon dioxide and epoxides. *ChemCatChem* **2016**, *8*, 234. [CrossRef]
12. Allen, S.D.; Moore, D.R.; Lobkovsky, E.B.; Coates, G.W. Highly-activity, single-site catalysts for the alternating copolymerization of CO_2 and propylene oxide. *J. Am. Chem. Soc.* **2002**, *124*, 14284. [CrossRef]
13. Kilic, A.; Durgun, M.; Ulusoy, M.; Tas, E. Conversion of CO_2 into cyclic carbonates in presence of metal complexes as catalysts. *J. Chem. Res.* **2010**, *2*, 622–626. [CrossRef]
14. Whiteoak, C.J.; Martin, E.; Belmonte, M.M.; Benet-Buchholz, J.; Kleij, A.W. An efficient iron catalysts for the synthesis of five- and six- membered organic carbonates under mild conditions. *Adv. Synth. Catal.* **2012**, *354*, 469. [CrossRef]
15. Whiteoak, C.J.; Kielland, N.; Laserna, V.; Castro-Gómez, F.; Martin, E.; Escudero-Adán, E.C.; Bo, C.; Kleij, A.W. Highly Active Aluminium Catalysts for the Formation of Organic Carbonates from CO_2 and Oxiranes. *Chem.—A Eur. J.* **2014**, *20*, 2264–2275. [CrossRef]
16. Paddock, R.L.; Nguyen, S.T. Chemical CO_2 Fixation: Cr(III) Salen Complexes as Highly Efficient Catalysts for the Coupling of CO_2 and Epoxides. *J. Am. Chem. Soc.* **2001**, *123*, 11498–11499. [CrossRef]
17. Buonerba, A.; de Nisi, A.; Grassi, A.; Milione, S.; Capacchione, C.; Vagin, S.; Rieger, B. Novel iron(III) catalyst for the efficient and selective coupling of carbon dioxide and epoxides to form cyclic carbonates. *Catal. Sci. Technol.* **2015**, *5*, 118–123. [CrossRef]
18. Andrea, K.A.; Butler, E.D.; Brown, T.R.; Anderson, T.S.; Jagota, D.; Rose, C.; Lee, E.M.; Goulding, S.D.; Murphy, J.N.; Kerton, F.M.; et al. Iron Complexes for Cyclic Carbonate and Polycarbonate Formation: Selectivity Control from Ligand Design and Metal-Center Geometry. *Inorg. Chem.* **2019**, *58*, 11231–11240. [CrossRef]
19. Srivastava, R.; Bennur, T.H.; Srinivas, D. Factors affecting activation and utilization of carbon dioxide in cyclic carbonates synthesis over Cu and Mn peraza macrocyclic complexes. *J. Mol. Catal. A Chem.* **2005**, *226*, 199–205. [CrossRef]
20. Man, L.M.; Lam, K.C.; Sit, W.N.; Ng, S.M.; Zhou, Z.; Lin, Z.; Lau, C.P. Synthesis of heterobimetallic Ru-Mn complexes and the coupling reactions of epoxides with carbon dioxide catalyzed by these complexes. *Chem.—A Eur. J.* **2006**, *12*, 1004–1015. [CrossRef]

21. Muñoz, B.K.; Viciano, M.; Godard, C.; Castillón, S.; García-Ruiz, M.; Blanco González, M.D.; Claver, C. Metal complexes bearing ONO ligands as highly active catalysts in carbon dioxide and epoxide coupling reactions. *Inorganica Chim. Acta.* **2021**, *517*, 120194. [CrossRef]
22. Zhang, X.; Jia, Y.-B.; Lu, X.-B.; Li, B.; Wang, H.; Sun, L.-C. Intramolecularly two-centered cooperation catalysis for the synthesis of cyclic carbonates from CO_2 and epoxides. *Tetrahedron Lett.* **2008**, *49*, 6589. [CrossRef]
23. Miao, C.-X.; Wang, J.-Q.; Wu, Y.; Du, Y.; He, L.-N. Bifunctional Metal-Salen Complexes as Efficient Catalysts for the Fixation of CO_2 with Epoxides under Solvent-Free Conditions. *ChemSusChem* **2008**, *1*, 236. [CrossRef] [PubMed]
24. Chang, T.; Jin, L.; Jing, H. Bifunctional chiral catalysts for the synthesis of chiral cyclic carbonates from carbon dioxide and epoxides. *ChemCatChem* **2009**, *1*, 379–383. [CrossRef]
25. Darensbourg, D.J. Making plastics from carbon dioxide: Salen metal complexes as catalysts to produce polycarbonates from epoxides and CO_2. *Chem. Rev.* **2007**, *107*, 2388–2410. [CrossRef]
26. Chatterjee, C.; Chisholm, M.H. The influence of the metal (Al, Cr, and Co) and the substituents of the porphyrin in controlling the reactions involved in the copolymerization of propylene oxide and carbon dioxide by porphyrin metal (III) complexes. 1. Aluminum chemistry. *Inorg. Chem.* **2011**, *50*, 4481–4492. [CrossRef]
27. Lu, X.-B.; Darensbourg, D.J. Cobalt catalysts for the coupling of CO_2 and epoxides to provide polycarbonates and cyclic carbonates. *Chem. Soc. Rev.* **2012**, *41*, 1462–1484. [CrossRef]
28. Darensbourg, D.J. Salen metal complexes as catalysts for the synthesis of polycarbonates from cyclic ethers and carbon dioxide. In *Synthetic Biodegradable Polymers*; Rieger, B., Kunkel, A., Coates, G.W., Reichardt, R., Dinjus, E., Zevaco, T.A., Eds.; Advances in Polymer Science; Springer: Berlin, Germany, 2012; Volume 245, pp. 1–27.
29. Chatterjee, C.; Chisholm, M.H. Influence of the metal (Al, Cr, and Co) and the substituents of the porphyrin in controlling the reactions involved in the copolymerization of propylene oxide and carbon dioxide by porphyrin metal(III) complexes. 2. Chromium chemistry. *Inorg. Chem.* **2012**, *51*, 12041–12052. [CrossRef]
30. Nakano, K.; Kamada, T.; Nozaki, K. Selective formation of polycarbonate over cyclic carbonate: Copolymerization of epoxides with carbon dioxide catalyzed by a cobalt(III) complex with a piperidinium end-capping arm. *Angew. Chem. Int. Ed.* **2006**, *45*, 7274–7277. [CrossRef]
31. Sujith, S.; Min, J.K.; Seong, J.E.; Na, S.J.; Lee, B.Y. A highly active and recyclable catalytic system for CO_2 propylene oxide copolymerization. *Angew. Chem. Int. Ed.* **2008**, *47*, 7306–7309. [CrossRef]
32. Ren, W.-M.; Liu, Z.-W.; Wen, Y.-Q.; Zhang, R.; Lu, X.-B. Mechanistics aspects of the copolymerization of CO_2 with epoxides using a thermally stable single-site cobalt (III) catalysts. *J. Am. Chem. Soc.* **2009**, *131*, 11509. [CrossRef] [PubMed]
33. Alexopoulou, K.I.; Zagoraiou, E.; Zafiropoulos, T.F.; Raptopoulou, C.P.; Psycharis, V.; Terzis, A.; Perlepes, S.P. Mononuclear anionic octahedral cobalt (III) complexes based on N-salicylidene-o-aminophenol and its derivatives: Synthetic, structural and spectroscopic studies. *Spectrochim. Acta Part A Mol. Biomol. Spectrosc.* **2015**, *136*, 122. [CrossRef] [PubMed]
34. Ghosh, P.; Chowdhury, A.R.; Saha, S.K.; Ghosh, M.; Pal, M.; Murmu, N.C.; Banerjee, P. Synthesis and characterization of redox non-innocent cobalt(III) complexes of a O,N,O donor ligand: Radical generation, semi-conductivity, antibacterial and anticancer activities. *Inorganica Chim. Acta* **2015**, *429*, 99. [CrossRef]
35. Abdel Aziz, A.A.; Salem, A.N.M.; Sayed, M.A.; Aboaly, M.M. Synthesis, structural characterization, thermal studies, catalytic efficiency and antimicrobial activity of some M(II) complexes with ONO tridentate Schiff base N-salicylidene-o-aminophenol (saphH2). *J. Mol. Struct.* **2012**, *1010*, 130. [CrossRef]
36. Belaid, S.; Landreau, A.; Djebbar, S.; Benali-Baitich, O.; Bouet, G.; Bouchara, J.P. Synthesis, characterization and antifungal activity of a series of manganese (II) and copper (II) complexes with ligands derived from reduced N,N′-O-phenylenebis(salicylideneimine). *J. Inorg. Biochem.* **2008**, *102*, 63–69. [CrossRef]
37. İspir, E.; Kurtoğlu, M.; Purtaş, F.; Serin, S. Synthesis and Antimicrobial Activity of New Schiff Bases Having the -SiOR Group (R = CH_3 or CH_2CH_3), and Their Transition Metal Complexes. *Transit. Met. Chem.* **2005**, *30*, 1042. [CrossRef]
38. Ueno, K.; Martell, A.E. Infrared studies on Synthetic Oxigen Carriers. *J. Phys. Chem.* **1956**, *60*, 1270–1275. [CrossRef]
39. Faniran, J.A.; Patel, K.S.; Bailar, J.C. Infrared spectra of N, N′-bis(salicylidene)-1,1-(dimethyl)ethylenediamine and its metal complexes. *J. Inorg. Nucl. Chem.* **1974**, *36*, 1547. [CrossRef]
40. Aranha, P.E.; dos Santos, M.P.; Romera, S.; Dockal, E.R. Synthesis, characterization, and spectroscopic studies of tetradentate schiff base chromium (III) complexes. *Polyhedron* **2007**, *26*, 1373–1382. [CrossRef]
41. Swamy, S.J.; Pola, S. Spectroscopic Studies on Co(II), Ni(II), Cu(II) and Zn(II) complexes with a N_4-macrocyclic ligands. *Spectrochim. Acta Part A Mol. Biomol. Spectrosc.* **2008**, *70*, 929–933. [CrossRef]
42. Sebastian, M.; Arun, V.; Robinson, P.P.; Varghese, A.A.; Abraham, R.; Suresh, E.; Yusuff, K.K.M. Synthesis, structural characterization and catalytic activity study of Mn(II), Fe(III), Ni(II), Cu(II) and Zn(II) complexes of quinoxaline-2-carboxalidine-2-amino-5-methylphenol: Crystal structure of the nickel (II) complex. *Polyhedron* **2010**, *29*, 3014–3020. [CrossRef]
43. Bailar, J.C.; Trotman-Dickenson, A.F. *Comprehensive Inorganic Chemistry*; Bailar, J.C., Emeleus, H.J., Nyholm, R., Trotman-Dickenson, A.F., Eds.; Pergamon Press: Oxford, UK, 1975; Volume 3, ISBN 9780080169880y0080169880.
44. Cotton, F.A.; Wilkinson, G.; Murillo, C.A.; Bochmann, M. *Advances in Inorganic Chemistry*, 6th ed.; Wiley: New York, NY, USA, 1999; ISBN 978-0-471-19957-1.

45. Cuesta-Aluja, L.; Castilla, J.; Masdeu-Bulto, A.M.; Henriques, C.A.; Calvete, M.J.F.; Pereira, M.M. Halogenated meso-phenyl Mn(III) porphyrins as highly efficient catalysts for the synthesis of polycarbonates and cyclic carbonates using carbon dioxide and epoxides. *J. Molec. Catal. A Chem.* **2016**, *423*, 489–494. [CrossRef]
46. Sônego Milani, J.L.; Moreira Meireles, A.; Noschang Cabral, B.; de Almeida Bezerra, W.; Terra Martins, F.; da Silva Martins, D.C.; das Chagas, R.P. Highly active Mn(III) meso-tetrakis(2,3-dichlorophenyl)porphyrin catalysts for the cycloaddition of CO_2 with epoxides. *J. CO_2 Util.* **2019**, *30*, 100–106. [CrossRef]
47. Kabsch, W. Integration, scaling, space-group assignment and post-refinement. *Acta Crystallogr. Sect. D* **2010**, *66*, 125–132. [CrossRef]
48. Burla, M.C.; Caliandro, R.; Carrozzini, B.; Cascarano, G.L.; Cuocci, C.; Giacovazzo, C.; Mallamo, M.; Mazzone, A.; Polidori, G. Crystal Structure Determination and Refinement via SIR2014. *J. Appl. Crystallogr.* **2015**, *48*, 306–309. [CrossRef]
49. Sheldrick, G. A short history of SHELX. *Acta Crystallogr. Sect. A Found. Crystallogr.* **2008**, *64*, 112. [CrossRef]
50. Farrugia, L. WinGX and ORTEP for Windows: An update. *J. Appl. Crystallogr.* **2012**, *45*, 849. [CrossRef]